FEBS Letters 587 (2013) 3681–3686

FEBS Letters

journal homepage: www.FEBSLetters.org

Inhibitor selectivity between aldo–keto reductase superfamily members AKR1B10 and AKR1B1: Role of Trp112 (Trp111)

Liping Zhang [a], Hong Zhang [a], Yining Zhao [a], Zhe Li [a], Shangke Chen [a], Jing Zhai [a], Yunyun Chen [a], Wei Xie [b], Zhong Wang [a], Qing Li [a], Xuehua Zheng [a,*], Xiaopeng Hu [a,*]

[a] School of Pharmaceutical Sciences, Centre for Cellular and Structural Biology of Sun Yat-sen University, Guangzhou 510006, China
[b] School of Life Sciences, Sun Yat-sen University, Guangzhou 510006, China

ARTICLE INFO

Article history:
Received 20 June 2013
Revised 10 September 2013
Accepted 25 September 2013
Available online 4 October 2013

Edited by Christian Griesinger

Keywords:
AKR1B10
AKR1B1
Inhibitor selectivity
Crystal structure

ABSTRACT

The antineoplastic target aldo–keto reductase family member 1B10 (AKR1B10) and the critical polyol pathway enzyme aldose reductase (AKR1B1) share high structural similarity. Crystal structures reported here reveal a surprising Trp112 native conformation stabilized by a specific Gln114-centered hydrogen bond network in the AKR1B10 holoenzyme, and suggest that AKR1B1 inhibitors could retain their binding affinities toward AKR1B10 by inducing Trp112 flip to result in an "AKR1B1-like" active site in AKR1B10, while selective AKR1B10 inhibitors can take advantage of the broader active site of AKR1B10 provided by the native Trp112 side-chain orientation.

1. Introduction

The NADPH dependent aldo–keto reductase (AKR) superfamily consists of around 150 critical phase I metabolizing enzymes that share high sequence similarities [1,2]. The failure of decades-long efforts to develop inhibitors of AKR1B1 (aldose reductase), which has been a leading drug target for type 2 diabetic complications since the 1990s, is partially related to adverse effects caused by cross-inhibition with other AKRs, such as AKR1A1 (aldehyde reductase, 65% sequence identity) [3,4]. AKR1B10, also called small intestine aldose reductase [5], is abnormally over-expressed in many malignant tumors [6], and could be responsible for carcinogenesis and chemoresistance by interrupting cell differentiation induced by retinoid acids [7], impairing cell apoptosis mediated by intracellular toxic carbonyls and isoprenyl aldehydes [8], and metabolizing anti-cancer drugs such as daunorubicin and idarubicin [9]. As a promising antineoplastic target, efforts have been expended on developing potent and specific AKR1B10 inhibitors [10–13].

Considering the 71% sequence identity and shared substrate specificity of AKR1B10 and AKR1B1, a clear understanding of inhibitor–enzyme interactions is essential for designing and screening specific AKR1B10/AKR1B1 inhibitors. Although over 100 crystal structures of AKR1B1 and its complexes with inhibitors have been determined, only one structure of AKR1B10 (in complex with a powerful AKR1B1 inhibitor tolrestat, PDB ID: 1ZUA) is available [7]. During the preparation of this manuscript, however, two more structures, e.g., AKR1B10 V301L mutant in complex with AKR1B1 inhibitors fidalrestat and sorbinil were reported (PDB ID: 4GAB and 4GA8, respectively) [14]. These AKR1B10 structures show almost identical inhibitor binding patterns to that of the corresponding AKR1B1–inhibitor complex structures (with tolrestat, fidarestat and sorbinil, PDB ID: 2FZD, 1EF3, 2PDK, respectively). However, this observed inhibitor binding pattern similarity cannot explain the specificity of selective AKR1B10 inhibitors, such as oleanolic acid [10] (Table 1 and Table S1 of the Supplementary data).

Here, we report the crystal structures of AKR1B10 holoenzyme (AKR1B10-$NADP^+$), its complexes with two AKR1B1 inhibitors (zopolrestat and epalrestat), one selective AKR1B10 inhibitor (flufenamic acid), and the AKR1B1-$NADP^+$–epalrestat complex (PDB ID: 4GQG, 4JII, 4JIH, 4I5X and 4JIR, see Table S2 for data collection and refinement statistics). These structures reveal a surprising Trp112 native conformation stabilized by a specific Gln114-centered hydrogen bond network in the AKR1B10 holoenzyme, and suggest that by inducing Trp112 flip to result in an "AKR1B1-like" active site in AKR1B10, some AKR1B1 inhibitors retain their binding affinities toward AKR1B10. Furthermore, these

Abbreviations: AKR1B10, aldo–keto reductase family1 member10; AKR1B1, aldose reductase aldo–keto reductase family1 member1; FLF, flufenamic acid; AKR1A1, aldehyde reductase

* Corresponding authors. Fax: +86 020 39943000.
E-mail address: huxpeng@mail.sysu.edu.cn (X. Hu).

0014-5793/$36.00
http://dx.doi.org/10.1016/j.febslet.2013.09.031

Table 1
Characteristics of inhibitors and crystal structures discussed in this work.

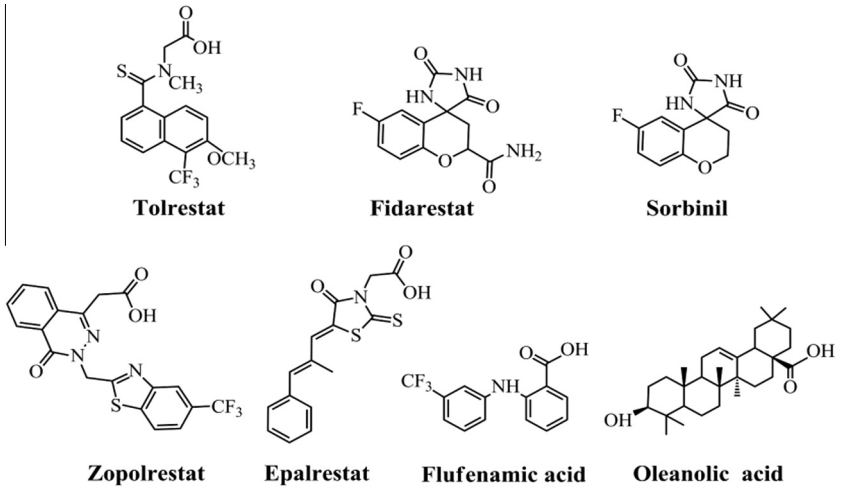

Enzymes inhibitors	IC_{50} (μM)				Trp112 conformation	Specificity pocket	
	B10	B1	B10 WT	B10 mut	B10	B10	B1
Tolrestat*	0.054	0.0014	n.d.	n.d.	B1-position (1ZUA)	Open	Open (2FZD)
Sorbinil*	9.6	0.55	n.d.	n.d.	B1-position (4GAB)	Open	Closed (2PDK)
Fidarestat*	33	0.026	n.d.	n.d.	B1-position (4GA8)	Open	Closed (1EF3)
Holoenzyme					B10-position (4GQG)	Closed	Closed* (1UZO)
Zopolrestat	0.62*	0.018*	0.17	0.36	B1-position (4JII)	Open	Open* (2FZ8)
Epalrestat	0.33*	0.021*	0.35	0.52	B10-position (4JIH)	Closed	Closed (4JIR)
Flufenamic acid	0.76*	41*	2.14	25	B10-position (4I5X)	Closed	Closed#
Oleanolic acid	0.09*	124*	0.8	14	B10-position#	Closed#	Closed#

(B10 WT, wide type AKR1B10; B10 mut, AKR1B10 Q114T/S304C double mutant.
n.d: not determined.
* Data from references.
# Predicated.

structures demonstrate that selective AKR1B10 inhibitors can take advantage of the broader active site of AKR1B10 provided by the native Trp112 side-chain orientation. The Trp112 (Trp111) side chain orientation of AKR1B10 (AKR1B1) thus could play a critical role in the determination of inhibitor selectivity between these two enzymes. These results provide an important structural basis for future drug development targeting AKR1B10 (AKR1B1).

2. Materials and methods

2.1. Materials and enzyme preparation

The enzyme was prepared using the method reported by Gallego [7]. Zopolrestat, flufenamic acid, epalrestat, and other reagents were purchased from Sigma–Aldrich.

2.2. Crystallization, data collection and structure determination

The AKR1B10-$NADP^+$ holoenzyme crystal was obtained at 289 K in hanging droplets consisting of protein solution mixed with a reservoir solution comprising 30–35% (w/v) PEG 6000 and 100 mM Tris-base (pH 9.0) at a 4:3 ratio. AKR1B10-$NADP^+$–inhibitor ternary complex crystals were prepared by co-crystallization. The crystal of the AKR1B1-$NADP^+$–epalrestat ternary complex was prepared as described previously [15]. X-ray diffraction data were collected at 100 K on an in-house Oxford Diffraction Xcalibur Nova diffractometer. The structures were determined with *CCP4* [16], *Phenix* [17] and *COOT* [18], while molecular docking was performed by *Discovery Studio* 2.5. All crystal structural figures were produced using *PyMOL*. Data collection and refinement statistics are summarized in Table S2.

3. Results and discussion

3.1. The structure of the AKR1B10 holoenzyme reveals a surprising Trp112 native conformation stabilized by a specific Gln114-centered hydrogen bond network

Structure superposition of our AKR1B10 holoenzyme and the previously reported AKR1B10–tolrestat complex structure reveals two significant differences in the conformations (overall r.m.s. deviation for 314 Cα atoms is 0.49 Å): (1) a different side-chain orientation of Trp112, and (2) a shift of Val301-Leu302-Gln303-Ser304 segment (Fig. 1B).

In the active site of the AKR1B10–tolrestat complex, Trp112 is located between the anionic site, formed by Tyr49, His111 and the nicotinamide moiety of $NADP^+$, and the so-called "specificity pocket" located at the interface of a loop consisting of Lys-125 to Ala-131 and the C-terminal loop (Fig. 1A). The Try112 side chain points to the anionic site. This orientation is the same as that of Trp111, the residue corresponding to Trp112 in all AKR1B1 structures. Although all other residues in the active site of the AKR1B10 holoenzyme structure generally overlap well with these in the AKR1B10–tolrestat complex structure, the side chain of Trp112 points to the "specificity pocket" instead. This Trp112 side chain orientation is therefore termed the "B10-position," while that of Trp112 in AKR1B10–tolrestat complex structure and Trp111 in AKR1B1 is termed the "B1-position".

Trp112 (Trp111) is a highly conserved residue in all known 14 AKR1B enzymes (Fig. S3). A careful check of the published structures for six AKR1B enzymes reveals that the corresponding residue Trp112 of AKR1B14 holoenzyme (rat aldose-reductase-like protein, PDB ID: 3O3R and 3QKZ) adopts the "B10-position" (Fig. S4) [19], while Trp111 of AKR1B4 (*Schistosoma japonicum*

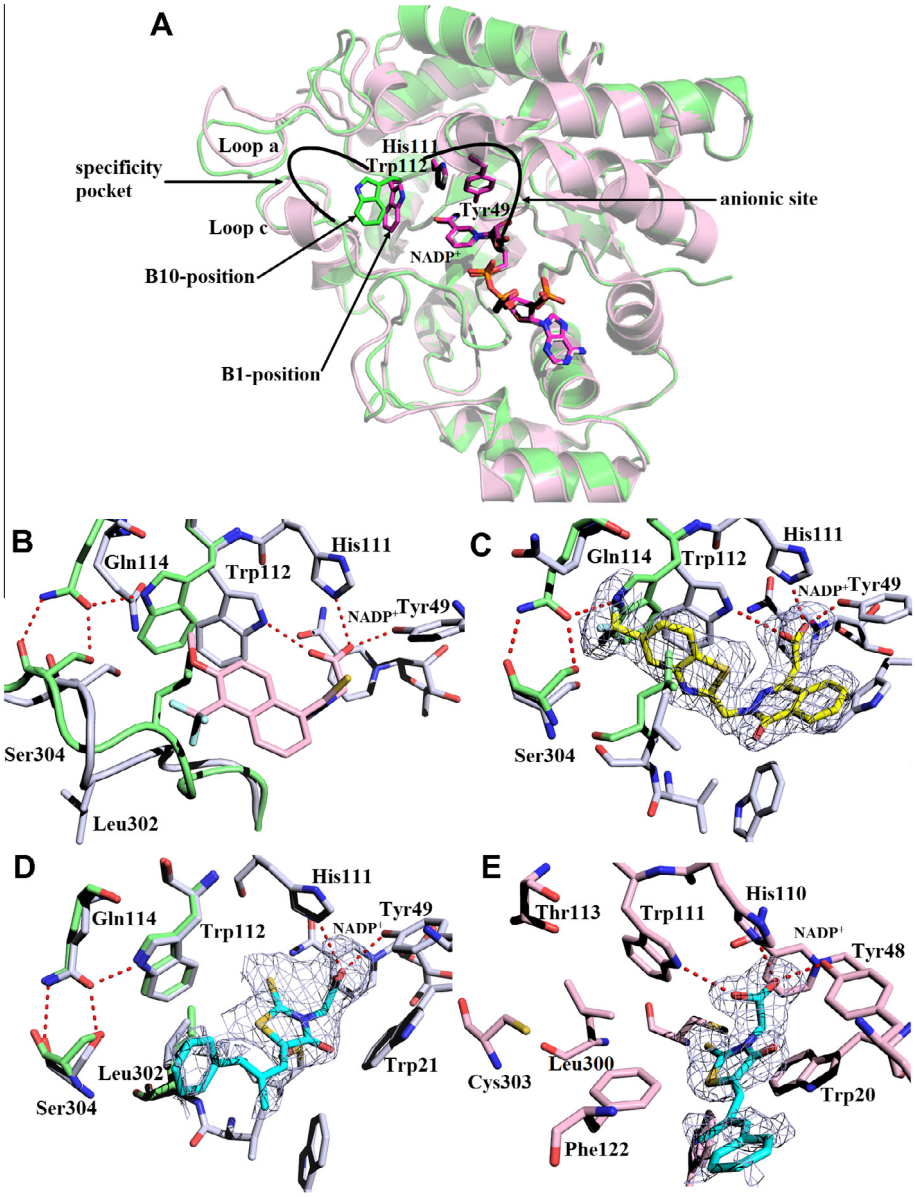

Fig. 1. Inhibitor-induced "specificity pocket" opening and change in the Trp112 side-chain conformation in AKR1B10. (A) Cartoon view of superimposed holoenzyme structures of AKR1B10 (green) and AKR1B1 (violet). Trp112 at the B10-position (green sticks) points to the specificity pocket, while Trp112 (Trp111) at the B1-position orients to the anionic pocket. (B–D): Superposition of the holo-AKR1B10 (green) active site structure with those of AKR1B10-tolrestat (grey and light pink), AKR1B10-zopolrestat (grey and yellow) and AKR1B10-epalrestat (grey and cyan), respectively. The F_o-F_c density maps are contoured in light blue at 2σ. Hydrogen bonds are shown as dashed red lines.

aldose reductase, PDB ID: 4HBK) holoenzyme and AKR1B8 bound with zopolrestat (fibroblast growth factor induced protein, PDB ID: 1FRB) adopt the "B1-position" [20,21]. In the holo-AKR1B9 structure (Chinese hamster ovary reductase, PDB ID: 1C9W), the corresponding residue (Trp111) is located at a transitional position between the "B1-position" and the "B10-position", Fig. S4) [22].

The conformation of "B10-position" Trp112 in the AKR1B10 holoenzyme is very likely to be stabilized by a specific hydrogen bond network centered on Gln114 (Gln114 ε^1O···Trp112 ε^1N 2.80 Å, Gln114 ε^1O···Ser304 OG 2.65 Å and Gln114 ε2N···Ser304 OG 2.73 Å, Fig. 1B). A similar hydrogen bond network (Trp112, Gln114 and Thr304) was observed in the AKR1B14 structure, while in AKR1B1/AKR1B4 structures, the corresponding residues (Trp111, Thr113 and Cys303 of AKR1B1, Trp111, Val113 and Met298 of AKR1B4) are not able to form a similar hydrogen bond network. For AKR1B9, the steric interaction of the Met306 side chain apparently restricts Gln113 (corresponding to Gln114 of AKR1B10) from forming a hydrogen bond network with Trp111 and Thr303. The "B1-position" of Trp111 in the AKR1B8–zopolrestat complex apparently results from binding of the inhibitor, as discussed below.

3.2. AKR1B1 inhibitor induced flip of Trp112 and formation of "AKR1B1-like" active site in AKR1B10 explains their activities toward AKR1B10

The coexistence of the shift of the Val301-Leu302-Gln303-Ser304 segment and the flip of Trp112 in AKR1B10–inhibitor structures is by no means coincidental. The shift of that segment is actually a result of opening of the "specificity pocket", a critical inhibitor induced sub-pocket in AKR1B1/inhibitor complex structures.

The AKR1B1 "specificity pocket" is primarily comprised of Thr113, Phe-115, Phe-122, Leu-300, Ser302 and Cys303, and is in

a closed state in the holoenzyme [23]. Upon binding of some AKR1B1 inhibitors, such as tolrestat [23] and zopolrestat [24], this "specificity pocket" changes to an open state to bind the hydrophobic portion of the inhibitors. This "specificity pocket" was believed to be essential for inhibitor selectivity between AKR1B1 and AKR1A1, since there is no such a pocket formed in AKR1A1 [23]. In the AKR1B10–tolrestat structure, a similar "specificity pocket" composed of Gln114, Phe116, Phe123, Val301, Gln303, and Ser304 was also observed, although at that time it was uncertain if this "specificity pocket" is really in the closed state in the holoenzyme [7].

The AKR1B10 holoenzyme structure shows that binding of tolrestat indeed induces the "specificity pocket" transformation from a closed to an open state. The shift of the Val301-Leu302-Gln303-Ser304 segment moves Ser304 and Leu302 away from their native positions, and results in collapse of the Gln114-centered hydrogen bond network. The loss of this stabilizing force causes a Trp112 side-chain flip, e.g., a switch of "B10-position" to "B1-position," and forms an "AKR1B1-like" active site in AKR1B10. A strong hydrogen bond (Nε1@Trp112 and Oε2@tolrestat, 2.81 Å) thus forms between the carboxylate group of tolrestat and Nε1 of Trp112 side chain, as is observed in the AKR1B1–tolrestat complex structure.

Other structures determined in this work support this inhibitor induced "AKR1B1-like" active site mechanism. Zopolrestat also opens the "specificity pocket" in AKR1B10, and induces formation of an "AKR1B1-like" active site in AKR1B10 (Fig. 1C). In contrast, the AKR1B1 inhibitor epalrestat, which does not result in an opening of the "specificity pocket" in AKR1B1, neither opens the "specificity pocket" nor induces an "AKR1B1-like" active site in AKR1B10. The same is true for the selective AKR1B10 inhibitor flufenamic acid (Figs. 1D, E and 2A).

The inhibitor induced "AKR1B1-like" active site mechanism explains the activities of the AKR1B1 inhibitors toward AKR1B10. For tolrestat and zopolrestat (and very likely all other AKR1B1 inhibitors with high AKR1A1 selectivity), the induced "AKR1B1-like" active site in AKR1B10 is consistent with strong inhibition of AKR1B10, while extra energy is required to induce an "AKR1B1-like" active site, making them weaker inhibitors toward AKR1B10 than AKR1B1. For cyclic imide based AKR1B1 inhibitors, minalrestat induces opening of the "specificity pocket" of AKR1B1 and strongly inhibits AKR1B10, while sorbinil cannot cause a flip of Trp112. Thus, the missing critical hydrogen bond between sorbinil and Trp111 in AKR1B1 explains the weak inhibition of sorbinil toward AKR1B10 [23,25–27]. On the other hand, the AKR1B1 inhibitor epalrestat also cannot induce an "AKR1B1-like" active site in AKR1B10, but unlike sorbinil, epalrestat can rotate its thiazolidinone plane by ca. 60° to fit in the active site of AKR1B10 (Fig. 1D and E). Therefore, epalrestat still strongly inhibits AKR1B10. The 1300-fold decreased activity of fidarestat towards AKR1B10 could be partially explained by a significant steric interaction (1.2 Å) between the Val301 side chain of AKR1B10 and the exocyclic amide of fidarestat, as revealed by overlap of the AKR1B1–fidarestat complex and the AKR1B10 holoenzyme structures. This explanation is supported by the 20-fold activity increment with the AKR1B10 V301L mutation [14]. Furthermore, the observation of Ruiz et al. that AKR1B10–fidarestat and AKR1B10–sorbinil complex structures could only be obtained via inhibitor replacement of AKR1B10 V301L-tolrestat crystals clearly indicates the importance of a preformed "AKR1B1 like" AKR1B10 induced by tolrestat [14].

3.3. A broader entrance to the anionic site in AKR1B10 due to the native Trp112 conformation explains the selectivity of rigid and bulky AKR1B10 inhibitors

The crystal structure of AKR1B10 in complex with flufenamic acid provides a straightforward structural basis for the generally rigid and bulky structures of selective AKR1B10 inhibitors. The native conformation of Trp112 (B10-position) results in a more accessible entrance to the anionic site in AKR1B10 than in AKR1B1, thus allowing the carboxylic group of flufenamic acid to occupy the anionic site and form critical hydrogen bonds with His111 ε2 N (2.86 Å), Tyr49 OH (2.57 Å) and Lys78 via a bridging water and close contact (3.28 Å) with the C4 atom of the coenzyme (Fig. 2A). Such interactions are unlikely to occur upon binding of flufenamic acid with AKR1B1 because of unfavorable steric interactions (ca. 2.4 Å) between the indole ring of Trp111 and the benzoic acid ring of flufenamic acid. As a result, flufenamic acid is a much weaker inhibitor toward AKR1B1 (IC_{50}: 41 μM vs. 0.76 μM, see Table 1).

In light of the increased accessibility of the anionic site in AKR1B10, we reexamined previously published molecular docking studies of the AKR1B10/oleanolic acid complex, which suggested that the 3β-hydroxyl group of oleanolic acid forms hydrogen bonds with anionic site residues (oleanolic acid O···His111 ε2N, 3.4 Å; oleanolic acid O···Tyr49 OH, 3.6 Å) [10]. Based on our crystal structure of AKR1B10–flufenamic acid, we found that the carboxylic group of oleanolic acid can be docked into the anionic site with two hydrogen bonds (oleanolic acid O2···Tyr49 OH, 2.8 Å; oleanolic acid O3···His111 ε2 N, 2.9 Å), and a normal electrostatic attraction with the nicotinamide of $NADP^+$ (Fig. 2B). Steric interactions between the 29- and 30-methyl groups of oleanolic acid and the Trp111 indole ring prevent the carboxylic group of oleanolic acid from inserting into the anionic binding site of AKR1B1 to form hydrogen bonds or electrostatic interactions with the co-factor. In

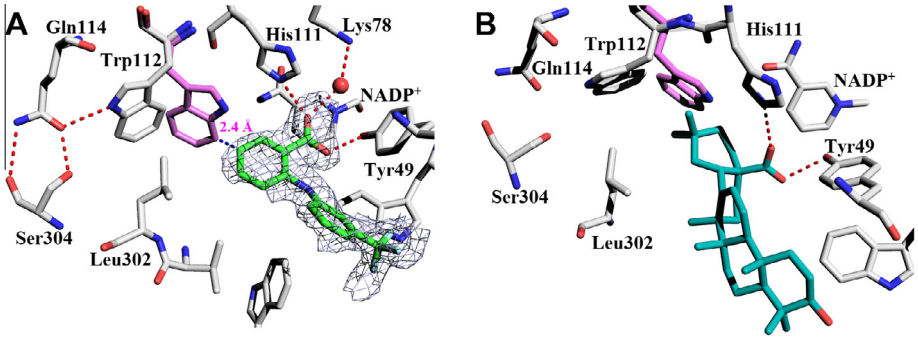

Fig. 2. Binding sites of (A) AKR1B10–flufenamic acid crystal structure and (B) AKR1B10–oleanolic acid docking model. Flufenamic acid: green, oleanolic acid: deep teal, AKR1B10: grey, Trp112 at B1-position: violet, hydrogen bond: red dashed line, unfavorable distance between flufenamic acid C3 and Trp112 Cz2: dashed blue line, water: red sphere. The F_o-F_c map is contoured in dark blue at 2σ for flufenamic acid.

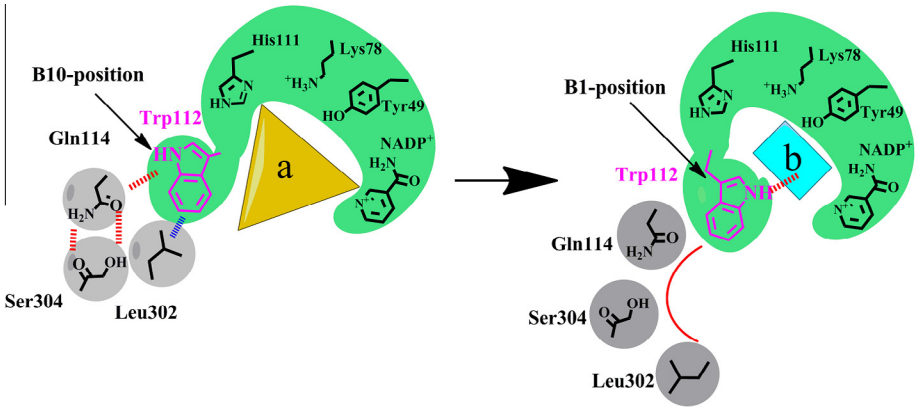

Fig. 3. Side chain orientation of Trp112 (Trp111) determines inhibitor selectivity between AKR1B10 and AKR1B1. Left: the AKR1B10 holoenzyme. Trp112 located at the B10-position leaves a wide entrance to the anionic site to accommodate selective AKR1B10 inhibitors with bulky and rigid scaffolds (yellow triangle a). Right: "AKR1B1-like" AKR1B10 active site. Some AKR1B1 inhibitors (blue quadrangle b) that induce opening of the "specificity pocket" (grey) and cause Trp112 to flip to the B1-position strongly inhibit AKR1B10.

contrast, in AKR1B10, the 29- and 30-methyl groups can strengthen oleanolic acid binding by forming hydrophobic contacts with Trp112. Thus, the binding mode not only coincides with the generally observed phenomenon that a strong hydrogen bond donating group is required for AKR1B10/AKR1B1 inhibitors to bind at the anionic site, but also provides a straightforward explanation for the high selectivity of oleanolic acid. Consistent with this hypothesis, erythrodiol, a derivative of oleanolic acid with the carboxyl group substituted by a hydroxyl group, exhibits very poor binding affinity toward AKR1B10 [10]. It also becomes clear why 5β-cholanic acid and isolithocholic acid are both highly selective AKR1B10 inhibitors, while 5β-cholanic acid methyl ester loses most of its binding ability towards AKR1B10 and AKR1B1 [28] (Table S5).

The binding modes of many other inhibitors listed in Table S1 are not known yet. However, the strong activities toward AKR1B10 and AKR1B1, but weak activity toward AKR1A1 of chromene-3-carboxamide derivatives [27], suggest that this type of compound triggers the "specificity pocket" opening and Trp112 flip to give an "AKR1B1-like" active site in AKR1B10. Furthermore, the apparent tendency of compounds such as γ-mangostin [29], curcumin [13], and 5α-pregnane-21-ol-3, 20-dione [28] to selectively inhibit AKR1B10 indicates that the increased accessibility of the anionic site of AKR1B10 is essential for their selectivity. To support this mechanism, we prepared the AKR1B10 Gln114Thr/Ser304Cys double mutant. These mutations are expected to loosen the Gln114-centered hydrogen bond network and allow the Trp112 side-chain to flip to the B1-position. As expected, flufenamic acid and oleanolic acid only inhibit this mutant very weakly, while zopolrestat and epalrestat are strong inhibitors of this mutant (Table 1).

4. Conclusion

As summarized in Table 1 and Fig. 3, the previously reported binding site geometry similarity between AKR1B1–inhibitor and AKR1B10–inhibitor complexes could be the result of inhibitor-induced "specificity pocket" opening and Trp112 side-chain flip at the active site of AKR1B10. The native conformations of Trp112 (Trp111) affect the inhibitor selectivity between AKR1B10 and AKR1B1. AKR1B1 inhibitors that are able to open the "specificity pocket" of AKR1B1 can also do so with AKR1B10 and induce a Trp112 side chain flip, resulting an "AKR1B1-like" active site in AKR1B10. Thus, these compounds are still good AKR1B10 inhibitors. AKR1B1 inhibitors that are not able to open the "specificity pocket" of AKR1B1 could be either good AKR1B10 inhibitors or not, depending on the flexibility of their structure. The wider entrance to the anionic site of AKR1B10 provided by the native Trp112 side chain orientation explains why selective AKR1B10 inhibitors are apt to be bulky and rigid molecules. Whether similar phenomena also occur in other AKRs–inhibitor interactions and how the subtle structural differences affect the screening and rational design of highly selective AKRs inhibitors are currently under study.

Acknowledgments

The authors gratefully thank a grant from the Natural Science foundation of China (No. 330004103041), and the Introduced Innovative R&D Team Leadership of Guangdong Province (PR China) (2011Y038) for financial support of this work. The authors also would like to thank Miss Jiazi Dinghe, a summer student from Beijing Haidian Foreign Language Shiyan School, Beijing, People's Republic of China, for her assistance.

Appendix A. Supplementary data

Supplementary data associated with this article can be found, in the online version, at http://dx.doi.org/10.1016/j.febslet.2013.09.031.

References

[1] Mindnich, R.D. and Penning, T.M. (2009) Aldo–keto reductase (AKR) superfamily: genomics and annotation. Human Genomics 3, 362–370.
[2] Penning, T.M. and Drury, J.E. (2007) Human aldo–keto reductases: function, gene regulation, and single nucleotide polymorphisms. Arch. Biochem. Biophys. 464, 241–250.
[3] Petrash, J.M. (2004) All in the family: aldose reductase and closely related aldo–keto reductases. Cell. Mol. Life Sci. 61, 737–749.
[4] Pastel, E., Pointud, J.C., Volat, F., Martinez, A. and Lefrancois-Martinez, A.M. (2012) Aldo–keto reductases 1b in endocrinology and metabolism. Front. Pharm. 3, 148.
[5] Cao, D., Fan, S.T. and Chung, S.S.M. (1998) Identification and characterization of a novel human aldose reductase-like gene. J. Biol. Chem. 273, 11429–11435.
[6] Kapoor, S. (2013) AKR1B10 and its emerging role in tumor carcinogenesis andas a cancer biomarker. Int. J. Cancer 132, 495.
[7] Gallego, O. et al. (2007) Structural basis for the high all-trans-retinaldehyde reductase activity of the tumor marker AKR1B10. Proc. Natl. Acad. Sci. U.S.A. 104, 20764–20769.
[8] Wang, C., Yan, R., Luo, D., Watabe, K., Liao, D.F. and Cao, D. (2009) Aldo–keto reductase family 1 member B10 promotes cell survival by regulating lipid synthesis and eliminating carbonyls. J. Biol. Chem. 284, 26742–26748.
[9] Matsunaga, T., Yamane, Y., Iida, K., Endo, S., Banno, Y., El-Kabbani, O. and Hara, A. (2011) Involvement of the aldo–keto reductase, AKR1B10, in mitomycin-c resistance through reactive oxygen species-dependent mechanisms. Anti-cancer Drugs 22, 402–408.

[10] Takemura, M. et al. (2011) Selective inhibition of the tumor marker aldo–keto reductase family member 1B10 by oleanolic acid. J. Nat. Prod. 74, 1201–1206.
[11] Soda, M. et al. (2012) Design, synthesis and evaluation of caffeic acid phenethyl ester-based inhibitors targeting a selectivity pocket in the active site of human aldo-keto reductase 1B10. Eur. J. Med. Chem. 48, 321–329.
[12] Endo, S., Matsunaga, T., Soda, M., Tajima, K., Zhao, H.T., El-Kabbani, O. and Hara, A. (2010) Selective inhibition of the tumor marker AKR1B10 by antiinflammatory N-phenylanthranilic acids and glycyrrhetic acid. Biol. Pharm. Bull. 33, 886–890.
[13] Matsunaga, T., Endo, S., Soda, M., Zhao, H.T., El-Kabbani, O., Tajima, K. and Hara, A. (2009) Potent and selective inhibition of the tumor marker AKR1B10 by bisdemethoxycurcumin: probing the active site of the enzyme with molecular modeling and site-directed mutagenesis. Biochem. Biophys. Res. Commun. 389, 128–132.
[14] Ruiz, F.X., Cousido-Siah, A., Mitschler, A., Farres, J., Pares, X. and Podjarny, A. (2013) X-ray structure of the V301L aldo–keto reductase 1B10 complexed with NADP(+) and the potent aldose reductase inhibitor fidarestat: implications for inhibitor binding and selectivity. Chemico-Biol. Interact. 202, 178–185.
[15] Zheng, X., Zhang, L., Zhai, J., Chen, Y., Luo, H. and Hu, X. (2012) The molecular basis for inhibition of sulindac and its metabolites towards human aldose reductase. FEBS Lett. 586, 55–59.
[16] Collaborative Computational Project, Number 4 (1994) The CCP4 suite: programs for protein crystallography. Acta Crystallogr. Section D: Biol. Crystallogr. 50, 760–763.
[17] Adams, P.D. et al. (2010) PHENIX: a comprehensive Python-based system for macromolecular structure solution. Acta Crystallogr. Section D: Biol. Crystallogr. 66, 213–221.
[18] Emsley, P. and Cowtan, K. (2004) Coot: model-building tools for molecular graphics. Acta Crystallogr. Section D: Biol. Crystallogr. 60, 2126–2132.
[19] Sundaram, K., Dhagat, U., Endo, S., Chung, R., Matsunaga, T., Hara, A. and El-Kabbani, O. (2011) Structure of rat aldose reductase-like protein AKR1B14 holoenzyme: Probing the role of His269 in coenzyme binding by site-directed mutagenesis. Bioorg. Med. Chem. Lett. 21, 801–804.
[20] Liu, J., Dyer, D.H., Cheng, J., Wang, J., Wang, S., Yang, Z., Wang, X. and Hu, W. (2013) Aldose reductase from *Schistosoma japonicum*: crystallization and structure-based inhibitor screening for discovering antischistosomal lead compounds. Parasit. Vectors 6, 162.
[21] Wilson, D.K., Nakano, T., Petrash, J.M. and Quiocho, F.A. (1995) 1.7 A structure of FR-1, a fibroblast growth factor-induced member of the aldo–keto reductase family, complexed with coenzyme and inhibitor. Biochemistry 34, 14323–14330.
[22] Ye, Q., Hyndman, D., Li, X., Flynn, T.G. and Jia, Z. (2000) Crystal structure of CHO reductase, a member of the aldo–keto reductase superfamily. Proteins 38, 41–48.
[23] Urzhumtsev, A. et al. (1997) A 'specificity' pocket inferred from the crystal structures of the complexes of aldose reductase with the pharmaceutically important inhibitors tolrestat and sorbinil. Structure 5, 601–612.
[24] Wilson, D.K., Tarle, I., Petrash, J.M. and Quiocho, F.A. (1993) Refined 1.8 A structure of human aldose reductase complexed with the potent inhibitor zopolrestat. Proc. Natl. Acad. Sci. U.S.A. 90, 9847–9851.
[25] Oka, M., Matsumoto, Y., Sugiyama, S., Tsuruta, N. and Matsushima, M. (2000) A potent aldose reductase inhibitor, (2*S*,4*S*)-6-fluoro-2′,5′-dioxospiro[chroman-4,4′-imidazolidine]-2-carboxamide (Fidarestat): its absolute configuration and interactions with the aldose reductase by X-ray crystallography. J. Med. Chem. 43, 2479–2483.
[26] El-Kabbani, O. et al. (2004) Ultrahigh resolution drug design. II. Atomic resolution structures of human aldose reductase holoenzyme complexed with Fidarestat and Minalrestat: implications for the binding of cyclic imide inhibitors. Proteins 55, 805–813.
[27] Endo, S., Matsunaga, T., Kuwata, K., Zhao, H.T., El-Kabbani, O., Kitade, Y. and Hara, A. (2010) Chromene-3-carboxamide derivatives discovered from virtual screening as potent inhibitors of the tumour maker, AKR1B10. Bioorg. Med. Chem. 18, 2485–2490.
[28] Endo, S. et al. (2009) Kinetic studies of AKR1B10, human aldose reductase-like protein: endogenous substrates and inhibition by steroids. Arch. Biochem. Biophys. 487, 1–9.
[29] Soda, M., Endo, S., Matsunaga, T., Zhao, H.T., El-Kabbani, O., Iinuma, M., Yamamura, K. and Hara, A. (2012) Inhibition of human aldose reductase-like protein (AKR1B10) by alpha- and gamma-mangostins, major components of pericarps of mangosteen. Biol. Pharm. Bull. 35, 2075–2080.